Metabolic oxidative stress elicited by the copper(II) complex [Cu(isaepy)2] triggers apoptosis in SH-SY5Y cells through the induction of AMP-activated protein kinase/p38MAPK/p53 signalling axis Evidence for a combined use with 3-bromopyruvate in neuroblastoma treatment

Giuseppe Filomeni, Simone Cardaci, Ana Maria da Costa Ferreira, Giuseppe Rotilio, Maria R Ciriolo

Biochemical Journal Immediate Publication. Published on 06 May 2011 as manuscript BJ20110510

Metabolic oxidative stress elicited by the copper(II) complex [Cu(isaepy)$_2$] triggers apoptosis in SH-SY5Y cells through the induction of AMP-activated protein kinase/p38^{MAPK}/p53 signalling axis

Evidence for a combined use with 3-bromopyruvate in neuroblastoma treatment

Giuseppe Filomeni[*,†], Simone Cardaci[*,†], Ana Maria Da Costa Ferreira[‡], Giuseppe Rotilio[*,§], and Maria Rosa Ciriolo[*,§,‖]

From: [*]Department of Biology, University of Rome "Tor Vergata", via della Ricerca Scientifica, 00133 Rome, Italy.
[‡]Departamento de Química Fundamental, Instituto de Química, Universidade de São Paulo, Av. Prof. Lineu Prestes 748, CEP 05508-900, São Paulo, SP, Brazil.
[§]Research Centre IRCCS San Raffaele Pisana, Via dei Bonacolsi, 00163, Rome, Italy.
[†]Both authors contributed equally to the work.
[‖]Address correspondence to: Maria Rosa Ciriolo, Department of Biology, University of Rome "Tor Vergata", Via della Ricerca Scientifica, 00133 Rome, Italy. Phone: +39 06 7259 4369 Fax: +39 06 7259 4311. E-mail: ciriolo@bio.uniroma2.it

Running title: *Anti-proliferative effects of [Cu(isaepy)$_2$] in SH-SY5Y cells.*

Keywords: delocalized lipophilic cations, AMPK, p38^{MAPK}, p53, copper complexes, 3-bromopyruvate, combined therapy, neuroblastoma.

Biochemical Journal Immediate Publication. Published on 06 May 2011 as manuscript BJ20110510

SYNOPSIS

We previously demonstrated that the complex bis[(2-oxindol-3-ylimino)-2-(2-aminoethyl)pyridine-N,N']copper(II), named [Cu(isaepy)$_2$], induces AMPK-dependent/p53-mediated apoptosis in tumour cells by targeting mitochondria. Here, we reveal that p38^{MAPK} is the molecular link of the phosphorylative cascade connecting AMPK to p53. Transfection of SH-SY5Y with a dominant negative mutant of AMPK results in apoptosis decrease, and a significant reduction of phospho-active p38^{MAPK} and p53. Similarly, reverse genetics of p38^{MAPK} yields a reduction of p53 and decreases apoptotic extent, confirming an exclusive hierarchy of activation that proceeds *via* AMPK/p38^{MAPK}/p53. Fuel supplies counteract [Cu(isaepy)$_2$]-induced apoptosis and AMPK/p38^{MAPK}/p53 activation, with glucose being the most effective, suggesting a role for energetic dysbalance in [Cu(isaepy)$_2$] toxicity. Co-administration of 3-bromopyruvate (3BrPA), a well-known inhibitor of glycolysis and succinate dehydrogenase, enhances apoptosis and AMPK/p38^{MAPK}/p53 signalling pathway activation. Under these conditions, no toxic effect is observed in superoxide dismutase-overexpressing SH-SY5Y, or in primary cortical neurons (PCN), which are, conversely sensitized to the combined treatment with [Cu(isaepy)$_2$] and 3BrPA only if grown in low glucose, or incubated with the glucose-6-phosphate dehydrogenase inhibitor, dehyroepiandrosterone. Overall, the results suggest that NADPH deriving from pentose phosphate pathway contributes to PCN resistance against [Cu(isaepy)$_2$] toxicity and propose its employment in combination with 3BrPA as possible tool for cancer treatment.

INTRODUCTION

AMP-activated protein kinase (AMPK) is a heterotrimeric serine/threonine protein kinase which acts as a fuel sensor in eukaryotic cells [1]. It is activated physiologically, when AMP:ATP ratio increases, and mediates the phosphorylation of a large number of metabolic enzymes aimed at the restoration of ATP levels. However, AMPK activation is enhanced under stress conditions associated with energetic dysbalance, such as glucose deprivation, hypoxia, and production of reactive oxygen species (ROS) [1-3]. Besides energy balance control, recent findings point out that AMPK-driven phosphorylative cascades can produce anti-proliferative effects in response to a variety of insults by inhibiting cell growth, slowing down cell cycle progression and promoting apoptosis [4-6]. Whereas AMPK-mediated cell growth inhibition mainly depends on the suppression of mTOR activity, which limits protein synthesis and activate autophagy [4, 7], cell cycle arrest and apoptosis induction seem to rely, at least in part, on p53 activation [8, 9]. AMPK-mediated p53 phospho-activation plays a crucial role either in the glucose-dependent regulation of a G_1/S metabolic checkpoint [10], or in the induction of apoptosis elicited by severe carbon source depletion and genotoxic stresses [8, 11]. Other pieces of evidence indicate that AMPK can also affect cell proliferation by the induction of apoptosis *via* the mitogen-activated protein kinases (MAPK) pathway, mainly those dependent on p38^{MAPK} and JNK. The former mediates the pro-apoptotic activity of AMPK upon UV and H_2O_2 exposure [8]; the latter is phospho-activated upon exposure to cannabinoid antagonists and in condition of sustained AMPK activation [12, 13]. Overall, these data suggest that AMPK can be considered as a molecular target of a feasible therapeutic strategy in cancer. Consistent with these observations, during the last years novel chemotherapeutics have been developed to affect selectively tumour growth and viability by promoting AMPK activation. For instance, several anti-diabetic drugs, such as metformin and the thienopyridone A769662, delay the growth of spontaneous tumours in AMPK responsive-manner [12-15]. Moreover, the evidence that the phosphatidylinositol ether lipid analogues (PIAs) and some natural compounds, such as curcumin and selenium, are able to elicit apoptosis in various cancer cell lines by activating AMPK [16-18], strengthens the idea that this kinase can represent a promising target both for anti-cancer and chemopreventive drugs.

Several studies demonstrate that cancer cells undergo a complex metabolic and bio-energetic reprogramming aimed at sustaining faster rate of growth and proliferation. This biochemical reorganization mainly consists in an increase of the glycolytic rate also under normal oxygen

tension (aerobic glycolysis or "Warburg effect"), which allows tumour cells using large amounts of glucose as carbon source for anabolic reactions [3, 19], and surviving under restrictive conditions [19, 20]. In accordance with this feature, ATP depleting molecules, such as the glycolytic inhibitors 2-deoxyglucose [21] and 3-bromopyruvate (3BrPA) [22], as well as several compounds able to affect oxidative phosphorylation (OXPHOS), have been exploited as tumour cell death inducers. Among them, delocalized lipophilic cations (DLCs), such as rhodamine 123, the thiopyrilium AA-1 and dequalinium chloride, due to their ability to selectively target mitochondria [23], are considered an efficient class of chemotherapeutics.

A chemotherapeutic strategy is to combine two or more drugs, which affect metabolic activity of cancer cells at low doses, in order to enhance their own killing properties and reduce side-effects on untrasformed healthy cells. For instance, the observation that many glycolytic inhibitors are able to improve the anticancer properties of several chemotherapeutics, including alkylating molecules [24], DNA intercalating agents [25] and DLCs [26, 27], reinforces the feasibility to develop novel anticancer therapies able to induce metabolic oxidative stress to overcome drug resistance and reduce systemic toxicity.

We previously characterized the pro-apoptotic activity of the bis[(2-oxindol-3-ylimino)-2-(2-aminoethyl)pyridine-N,N']copper(II), named [Cu(isaepy)$_2$], an isatin-Schiff base copper(II) complex highly efficient in inducing neuroblastoma and carcinoma cell death [28, 29]. We demonstrated that [Cu(isaepy)$_2$] behaves as an uncoupler and a DLC-like molecule that yields oxidative damages in the mitochondrial compartment. In this work we have deeply dissected the signalling pathways responsible for the final induction of [Cu(isaepy)$_2$]-induced apoptosis in SH-SY5Y cells, highlighting the role of the energetic stress-responsive pathway AMPK/p38^{MAPK}/p53 as the principal route governing the apoptotic response. In addition, we have provided evidence supporting the putative use of this copper-based complex in combination with 3BrPA as a feasible therapeutic strategy for neuroblastoma treatment.

MATERIALS AND METHODS

Materials – Isatin-diimine copper(II) complex bis[(2-oxindol-3-ylimino)-2-(2-aminoethyl)pyridine-N,N']copper(II) perchlorate, [Cu(isaepy)$_2$](ClO$_4$)$_2$, named *[Cu(isaepy)$_2$]*, was synthesized as previously described [28, 30]. 3-bromopyruvate (3BrPA), dihydroepiandrosterone (DHEA), dimethyl sulfoxide (DMSO), dithiothreitol (DTT), glucose, methyl-succinate, paraformaldehyde, propidium iodide, retinoic acid (RA), rhodamine 123 (Rho123), sodium pyruvate, Triton X-100 were from Sigma (St. Louis, MO). Dequalinium chloride (DQC) was from Alexis (Lausen, Switzerland). 2',7'-dichlorodihydrofluorescein diacetate (H_2DCF-DA) and 2-[N-(7-nitrobenz-2-oxa-1,3-diazol-4-yl) amino]-2-deoxy-D-glucose (2-NBDG) were from Invitrogen (San Giuliano Milanese, Italy). Goat anti-mouse IgG (H+L)-horseradish peroxidase-conjugate was from Bio-Rad Lab. (Hercules, CA). N-Tris(hydroxymethyl)methyl-2-aminoethanesulfonic acid (TES) was from US Biological (Cleveland, OH). All other chemicals were from Merck (Darmstadt, Germany).

SH-SY5Y cells cultures – Human neuroblastoma SH-SY5Y cells were grown in D-MEM/F12 supplemented with 10% fetal calf serum, glutamine and penicillin/streptomycin and cultured at 37 °C in an atmosphere of 5% CO_2 in air. During the experiments, cells were plated at a density of 4 × 10^4/cm^2, unless otherwise indicated. SH-SY5Y overexpressing the WT form of the human superoxide dismutase 1 (*h*SOD cells) were obtained as previously described [28].

Primary mouse cortical neurons – Mouse primary cortical neurons (PCN) were obtained from cerebral cortices of E15 C57BL-6 mice embryos. All the experiments were performed according to the Animal Research Guidelines of the European Communities Council Directive (86/609/EEC). Minced cortices were digested with trypsin (Lonza) 0.25% - EDTA at 37 °C for 7 minutes. Cells were stained with 0.08% Trypan blue solution and only viable cells were counted and plated at the density of 1 x 10^5/cm^2 onto poly-D-lysine coated coverlips or multiwell plates in 5 mM (low glucose, *LG*) or 25 mM glucose-containing MEM medium supplemented with 10% fetal bovine serum, 2 mM glutamine, and 0.1 mg/ml gentamicin (Invitrogen). After 1h, the medium was

replaced with Neurobasal medium containing antioxidant-free B27 supplement (Invitrogen), 2 mM glutamine and 0.1 mg/ml gentamicin. Cell cultures were kept at 37 °C in a humidified atmosphere containing 5% CO_2. Every 3 days, one third of the medium was replaced up to day 7, time at which the cells were treated.

Transfections – Twenty-four hours after plating, 50% confluent SH-SY5Y cells were transfected with a SignalSilence® Pool $p38^{MAPK}$ siRNA ($sip38_1$) (Cell Signalling Technology, Beverly, MA) or with a ON-TARGET*plus* $p38^{MAPK}$ siRNA ($sip38_2$, Thermofisher Scientific-Dharmacon, Lafayette, CO). Control cells were transfected with a scramble siRNA duplex, which does not present homology with any other human mRNAs (siScr). Over-expression of mutated proteins were carried out by transfecting the cells with a pcDNA3 empty vector or with a pcDNA3 vector containing: *i*) the myc-tagged coding sequence for the α2 subunit of AMPK carrying the T→A substitution at the residue 172 (kindly provided by Prof. David Carling from the Clinical Sciences Centre, Imperial College, Hammersmith Hospital, Du Cane Road, London, UK); *ii*) the flag-tagged coding sequence for the α1 subunit of $p38^{MAPK}$ carrying loss-of-function mutation in the catalytic residues (kinase mutant, *KM*, kindly provided by Prof. Jiahuai Han, from The Scripps Research Institute, Department of Immunology, North Torrex Pines Road, La Jolla, CA, USA). After transfection, cells were immediately seeded into fresh medium and used after 48 h, because this time was sufficient to significantly increase the expression of these dominant/negative forms of the proteins. Cells were transfected by electroporation using a Gene Pulser Xcell system (Bio-Rad) according to the manufacturer's instructions and directly seeded into fresh medium. Transfection efficiency was estimated by co-transfecting siRNA or plasmids with non-specific rhodamine-conjugated oligonucleotides and found to be > 80 %.

Treatments – A 5 mM solution of $[Cu(isaepy)_2]$ was prepared just before the experiments by dissolving the lyophilized compounds in DMSO. Treatments were performed in serum-supplemented media with $[Cu(isaepy)_2]$ at the final concentration of 50 μM, unless otherwise stated. DQC and Rho123 were dissolved in PBS and DMSO, respectively, and employed at the concentration of 100 μM. The p53 inhibitor pifithrin-α was dissolved in DMSO and used at 20 μM. Fuel supplies were dissolved in PBS and added to the medium to reach the final concentration of 30 mM glucose, 10 mM sodium pyruvate or 10 mM methyl-succinate. The glucose-6-phosphate dehydrogenase inhibitor DHEA was dissolved in DMSO and administered at the final concentration of 1 μM. 3BrPA was dissolved in PBS and used alone or in combination with $[Cu(isaepy)_2]$ at the concentration of 10 μM. Retinoic acid (RA) was dissolved in DMSO and used at the concentration of 20 μM in order to induce differentiation of SH-SY5Y cells and re-added routinely for a two-week period. All the treatments were maintained throughout the treatment with $[Cu(isaepy)_2]$. As control, equal volumes of PBS (for DQC, 3BrPA and fuel supplies) or DMSO (for the remaining compounds) were added to cell medium.

Cell viability – Cell viability was estimated by direct count upon Trypan blue exclusion. For the evaluation of apoptosis, cells were stained with 50 μg/ml propidium iodide prior to analysis by a FACScalibur instrument (BD Biosciences, San José, CA). The percentages of apoptotic cells were evaluated as previously described [31].

Measurement of ROS and carbonylated protein levels – Detection of intracellular ROS and protein carbonyls was performed as previously described [28]. Briefly, cells were incubated with 50 μM H_2DCF-DA (dissolved in DMSO) for 2 h at 37°C, then treated with $[Cu(isaepy)_2]$ and fluorescence of DCF, generated upon reaction with ROS, analyzed cytofluorometrically. Treatment with 100 μM *tert*-butyl hydroperoxide was used as a positive control. Carbonylated proteins were detected using the Oxyblot Kit (Intergen, Purchase, NY) after reaction with 2,4-dinitrophenylhydrazine (DNP) for 15 min at 25 °C. Samples were resolved on 12% SDS-polyacrylamide gels and DNP-derivatized proteins were identified by immunoblot using an anti-DNP antibody.

Measurement of 2-NBDG uptake – Cells were incubated for 1 h with 100 μM 2-NBDG (dissolved in DMSO), a fluorescent derivative of 2-deoxy-D-glucose, washed with PBS, collected and analyzed cytofluorometrically [32].

Extracellular lactate assay – Extracellular lactate concentration was assessed as previously described [33]. Briefly, 10 μl of trichloroacetic acid-precipitated proteins from cell media was incubated at room temperature in 290 μl of a 0.2 M glycine/hydrazine buffer, pH 9.2, containing 0.6 mg/ml NAD^+ and 17 U/ml lactate dehydrogenase. NAD^+ reduction was followed at 340 nm and nmoles of NADH formed were considered stoichiometrically equivalent to extracellular lactate.

Western blot analyses – Total lysates and mitochondrial enriched fraction from SH-SY5Y cells were obtained as previously described [24]. Proteins were electrophoresed by SDS-PAGE and blotted onto nitrocellulose membrane (Bio-Rad). Monoclonal anti-SOD1 and anti-Hsp60 (Santa Cruz Biotechnology) were used as loading/purity control of cytosolic and mitochondrial fractions, respectively. Monoclonal anti-p53 (clone BP5312) and anti-actin (Sigma); anti-phospho-thr172 of AMPK α-subunits (Cell Signalling Technology); anti-glyceraldehyde-3-phosphate dehydrogenase (GAPDH, Santa Cruz Biotechnology, Santa Cruz, CA), or polyclonal anti-AMPK, anti-Bax and anti-$p38^{MAPK}$ (Santa Cruz Biotechnology); anti phospho-thr180/tyr182 $p38^{MAPK}$ (Invitrogen, San Giuliano Milanese, Italy) were used as primary antibodies. The specific protein complex, formed upon specific secondary antibody treatment, was identified using a Fluorchem Imaging system (Alpha Innotech, M-Medical, Milano, Italy) after incubation with ChemiGlow chemoluminescence substrate (Alpha Innotech). The protein complex, formed upon the reaction with specific secondary antibodies, was identified using a FluorChem Imaging System (Alpha Innotech, M-Medical, Milano, Italy) after the incubation with ChemiGlow chemoluminescence substrate (Alpha Innotech). Densitometric analyses were calculated using Quantity One Software (Bio-Rad).

Protein Determination – Proteins were determined by the method of Lowry et al [34].

Data presentation – All experiments were done at least five different times unless otherwise indicated. The results are presented as means ± SD. Statistical evaluation was conducted by ANOVA, followed by correction with Bonferroni's test. Comparisons were considered to be significant at $p < 0.05$.

RESULTS AND DISCUSSION

AMPK is upstream of $p38^{MAPK}$ and p53 in the phosphorylative cascade culminating in [Cu(isaepy)$_2$]-induced apoptosis. – A tight reliance between AMPK and $p38^{MAPK}$ in the phosphorylative cascade leading to energetic/oxidative stress-dependent apoptosis is emerging [8, 18], and a $p38^{MAPK}$-dependent phospho-activation of p53 can occur upon chemical and physical stresses [18, 33, 35]. Previously, we demonstrated that [Cu(isaepy)$_2$]-mediated cell death in SH-SY5Y was associated with AMPK and p53 up regulation [28, 29], therefore, we asked whether AMPK and p53 activation were events correlated by the intermediate induction of $p38^{MAPK}$. To this aim, we analyzed their expression and phosphorylative levels upon treatment with 50 μM of [Cu(isaepy)$_2$] (**Fig. 1A**). Although the basal levels of AMPK and $p38^{MAPK}$ remained unchanged during the treatment, phospho-AMPK and phospho-$p38^{MAPK}$, as well as p53, rapidly increase as soon as 1 h after [Cu(isaepy)$_2$] addition (**Fig. 1B**). Moreover, further analyses indicated that these effects were dose dependent in the micromolar range (see **Suppl. Fig. 1**). To verify whether $p38^{MAPK}$ and p53 were AMPK-responsive factors, we took advantage of cells overexpressing the non-phosphorylable dominant/negative form (T172A) of the α2 subunit of AMPK (AMPK D/N cells), treated them with [Cu(isaepy)$_2$] and evaluated whether p53 and phospho-$p38^{MAPK}$ were modulated in these conditions. Consistent with our previous results [29], cytofluorometric analyses shown in **Fig. 1C** indicate that AMPK D/N were resistant to [Cu(isaepy)$_2$]-induced apoptosis. Compared to normal cells, a lower, but still measurable, activation of both $p38^{MAPK}$ and p53 was also observed under these conditions (**Fig. 1D**). To confirm the tight dependence of $p38^{MAPK}$ and p53 activation on AMPK-phosphorylation, we evaluated the localization of phospho-$p38^{MAPK}$ and

p53 in AMPK D/N cells by fluorescence microscopy. **Fig. 1E** shows that, in line with the above reported results, the nuclear localization of both $p38^{MAPK}$ and p53 was reduced in cells where AMPK phospho-activation was prevented. These results suggested that the activation of AMPK and $p38^{MAPK}$ were joined each other along a unique phosphorylative cascade governing cell response to [Cu(isaepy)$_2$] and culminating in p53-dependent cell death.

$p38^{MAPK}$ mediates [Cu(isaepy)$_2$] toxicity and regulates p53 activation – p53 gains transcriptional activity downstream of phosphorylative events mediated by different protein kinases, such AMPK and $p38^{MAPK}$ [8, 9, 18]. To establish whether p53 was an exclusive target of AMPK or $p38^{MAPK}$, we knocked down $p38^{MAPK}$ by siRNA technique and analyzed both cell death and p53 expression levels upon 24 h-treatment with 50 μM [Cu(isaepy)$_2$]. **Fig. 2A** shows cytofluorometric analyses, upon staining with propidium iodide, of SH-SY5Y cells transfected with two alternative siRNAs against $p38^{MAPK}$ (*sip38$_1$* and *sip38$_2$* cells) or with a scramble 21-nucleotide RNA sequence (*siScr* cells). In particular, data indicated that both sip38 cells showed a lesser extent of subG1 (apoptotic) population than siScr counterparts, with sip38$_1$ cells being more resistant to [Cu(isaepy)$_2$]-induced toxicity. In line with this result, no increase of p53 immunoreactivity was observed in sip38$_1$ cells at each time point examined (**Fig. 2B**), indicating that p53 activation depended only on $p38^{MAPK}$. Similar results were also obtained in cells overexpressing the kinase inactive mutant of $p38^{MAPK}$ (*p38-KM* cells), which is still activable by upstream kinases, but is unable to phosphorylate downstream targets. **Fig. 2C** shows that p38-KM cells were significantly rescued from [Cu(isaepy)$_2$]-induced apoptosis. Consistent with this observation, despite a sustained increase of the immunoreactivity of phospho-$p38^{MAPK}$, no significant increment of p53 expression levels was obtained (**Fig. 2D**), suggesting that, upon treatment with [Cu(isaepy)$_2$], $p38^{MAPK}$ was the molecular link between AMPK and p53.

AMPK/$p38^{MAPK}$/p53 signalling axis is responsive to [Cu(isaepy)$_2$]-mediated energetic impairment. – We reported that [Cu(isaepy)$_2$] induces oxidative phosphorylation dysfunction, which finally leads to mitochondrial trans-membrane potential ($\Delta\Psi_m$) loss and ATP decrease [29]. To assess whether the activation of AMPK/$p38^{MAPK}$/p53 signalling pathway relied upon [Cu(isaepy)$_2$]-mediated energetic impairment, we incubated the cells with fuel supplies that enter metabolic pathways at different points: 30 mM glucose, 10 mM pyruvate and 10 mM succinate, as the esterified form of methyl succinate. Then the cells were treated with 50 μM [Cu(isaepy)$_2$] for 24 h and apoptosis evaluated cytofluorometrically. **Fig. 3A** shows that, although at different extent, these compounds decreased the percentage of apoptotic cells. It is also worth noting that the extents of apoptotic cells measured upon glucose and succinate incubation were significantly lower than those evaluated upon pyruvate addition, confirming that ATP deriving from glycolysis, or generated bypassing mitochondrial Complex I was sufficient, at least in part, to counteract [Cu(isaepy)$_2$]-mediated energetic stress and apoptosis. Therefore, we performed Western blot analyses of phospho-$p38^{MAPK}$ and p53 under the same conditions. **Fig. 3B** shows that glucose and succinate addition decreased phospho-$p38^{MAPK}$ and p53 immunoreactivity to an extent correlating with their capability to rescue cells from death. Conversely, pyruvate only faintly countered AMPK/$p38^{MAPK}$/p53 activation, in a way resembling the weak protection exerted against [Cu(isaepy)$_2$]-induced apoptosis.

It has been recently demonstrated that retinoic acid (RA) enhances metabolic stress-stimulated glucose uptake in skeletal muscle cells [37]. Since we previously found that RA incubations completely rescued cells from [Cu(isaepy)$_2$]-induced apoptosis [28], we wondered whether this event was mediated by an increase of glucose uptake and a consequent modulation of AMPK-dependent signalling axis. We then analyzed whether RA influenced glucose uptake in SH-SY5Y cells by evaluating cytofluorometrically the incorporation of 2-NBDG, a fluorescent analogue of the non-phosphorylable 2-deoxyglucose. **Fig. 3C** shows that, incubation with RA significantly increased 2-NBDG uptake, confirming that this process is active also in SH-SY5Y.

Next, the cells were incubated with 20 μM RA, treated with 50 μM [Cu(isaepy)$_2$] and the activation of AMPK/p38^{MAPK}/p53 pathway analyzed by Western blot. **Fig. 3D** shows that RA incubation prevented the accumulation of phospho-AMPK and phospho-p38, as well as of p53. Results obtained by this set of experiments were consistent with the idea that [Cu(isaepy)$_2$] induced metabolic stress, and confirmed that either cell re-feeding with different fuel supplies, or increase of glucose uptake reduced [Cu(isaepy)$_2$]-induced cytotoxicity by weakening the activation of AMPK/p38^{MAPK}/p53 signalling pathway.

AMPK/p38^{MAPK}/p53 axis is not a prototype of DLCs-responsive signalling pathway. – Since we characterized [Cu(isaepy)$_2$] as a molecule belonging to the DLCs class, we wondered whether the activation of AMPK/p38^{MAPK}/p53 axis was specific for [Cu(isaepy)$_2$], or a general cell response towards other DLCs differently affecting mitochondrial function. To this aim, we selected dequalinium chloride (DQC) and rhodamine 123 (Rho123), the former specifically targeting Complex I and the latter affecting F_0/F_1-ATPase activity. After dose-response experiments (data not shown), we chose the concentration of 100 μM for both compounds because it showed an extents of apoptosis similar to those achieved with [Cu(isaepy)$_2$]. Indeed, after 24 h-treatment with both DQC and Rho123, SH-SY5Y cells underwent cell death with percentages of about 30% (**Fig. 4A**). This phenomenon well correlated with an increase of immunoreactivity of p53 (**Fig. 4B**) after 6 and 12 h-treatment, suggesting that p53 could be associated with cell death mechanisms downstream of mitochondrial dysfunction. However, no phospho-activation of AMPK and p38^{MAPK} was observed (**Fig. 4B**), indicating that this signalling axis was specific for [Cu(isaepy)$_2$]. To validate these assumptions, we incubated the cells with 20 μM pifithrin-α, the chemical inhibitor of p53 or, alternatively, over expressed the inactive form AMPK D/N, and then analyzed the extent of apoptosis after 24 h-treatment with 100 μM Rho123 and DQC. As shown in **Fig. 4C**, no protection against Rho123 and DQC-induced toxicity was achieved in both the experimental conditions, indicating that AMPK/p38^{MAPK}/p53 signalling pathway is exclusive for [Cu(isaepy)$_2$], whereas different mechanisms are involved in cell death induction downstream of conventional DLCs.

3BrPA enhances [Cu(isaepy)$_2$] cytotoxicity by the enhancement of a metabolic oxidative stress – One of the main purposes of cancer therapy is to be less aggressive towards normal tissues, but efficient enough to kill transformed cells, and avoid cell resistance. To reach this goal, a combined therapy is often used. Therefore, we attempted to decrease the concentration of [Cu(isaepy)$_2$] down to doses that, *per se*, do not induce apoptosis and employed it in combination with the glycolytic inhibitor 3BrPA, which eradicates liver cancer in animals without associated systemic toxicity [38]. 3BrPA was discovered as an efficient inhibitor of hexokinase II [39, 40], and only recently characterized to affect also succinate dehydrogenase activity [41], thus providing the molecular bases of its anti-tumour property. **Fig. 5A** shows that SH-SY5Y cells underwent apoptosis when 10 μM [Cu(isaepy)$_2$] and 10 μM 3BrPA were used in combination, while no toxicity was evidenced when the same concentrations of [Cu(isaepy)$_2$] and 3BrPA were administered separately. To assess whether, AMPK/p38^{MAPK}/p53 signalling axis was activated also under these conditions, we performed Western blot analyses of the expression levels of these proteins. **Fig. 5B** shows that the phosphorylated form of AMPK, p38^{MAPK} and the protein levels of p53 significantly increased only upon the combined treatment, whereas they remained unchanged when [Cu(isaepy)$_2$] and 3BrPA were used alone.

Taken together these preliminary results indicated that the addition of 3BrPA, a further energy depleting molecule, allowed to decrease the concentrations of [Cu(isaepy)$_2$], and to achieve the same toxic effects in neuroblastoma cells. We then moved to primary cortical neurons (PCN) to evaluate the toxic effects of [Cu(isaepy)$_2$]. In particular, incubations with 50 μM [Cu(isaepy)$_2$] for 24 h yielded widespread cell death with the feature of necrosis (data not shown), indicating that [Cu(isaepy)$_2$] was toxic even in untransformed cells when used at high doses. This observation

prompted us to perform combined treatments with low doses of both [Cu(isaepy)$_2$] and 3BrPA in order to minimize their side-effects in healthy cells. To verify whether these conditions were tolerated by PCN, we treated the cells with 10 μM [Cu(isaepy)$_2$] and/or 10 μM 3BrPA for 24 h and analyzed apoptosis induction by counting condensed/fragmented nuclei upon Hoechst 33342 staining and by evaluating caspase-3 cleavage through fluorescence microscopy. **Figs. 5C** and **5D** show that, differently from observed in SH-SY5Y cells, neither upon single treatment nor in combination, [Cu(isaepy)$_2$] and 3BrPA, at low doses, induced a significant activation of apoptosis. To assess whether this different sensitivity was associated with the different glycolytic metabolism between SH-SY5Y and PCN, we next analyzed the extracellular lactate concentration, which is a suitable marker of the glycolysis. **Fig. 5E** indicates that PCN had a much lower glycolytic rate than the neuroblastoma counterpart, which was corroborated by the evidence of a 10-fold less basal levels of lactate in the extracellular space. Moreover, in PCN, lactate production was not affected by treatment with [Cu(isaepy)$_2$] or 3BrPA, whereas it underwent significant decrease when SH-SY5Y were treated with 3BrPA, indicating that by inhibiting the tumour specific isoform hexokinase II, 3BrPA mainly affects glycolytic metabolism of neuroblastoma and result virtually ineffective in PCN. This result indicated that a metabolic stress could be implicated in the apoptotic response of neuroblastoma cells to the combined treatment with [Cu(isaepy)$_2$] and 3BrPA, although it revealed mainly depended on the contribution of 3BrPA.

To assess the role of oxidative stress in the toxicity of the combined treatment, we evaluated relative ROS production upon incubation with H_2DCF-DA. **Fig. 6A** shows that [Cu(isaepy)$_2$] and 3BrPA yielded intracellular ROS increase in SH-SY5Y cells when employed alone or in combination, whereas, only a very mild, although significant, effect was observed in PCN. To deeply investigate this issue, we took advantage of an SH-SY5Y cell line overexpressing the WT form of the human antioxidant enzyme SOD1 (*h*SOD cells) [28]. Both parental and SOD1 overexpressing SH-SY5Y were treated with 10 μM [Cu(isaepy)$_2$] in the presence of 10 μM 3BrPA for 24 h, and apoptosis was then analyzed cytofluorometrically. **Fig. 6B** shows that, under these conditions, the percentage of apoptosis was halved in *h*SOD cells, and the levels of phospho-AMPK, phospho-p38^{MAPK}and p53 were reduced (**Fig. 6C**). This result clearly indicated that the different susceptibility correlated with a different degree of activation of the AMPK/p38^{MAPK}/p53 signalling axis, and concomitantly suggested that, besides the energetic impairment, oxidative stress taking place downstream of [Cu(isaepy)$_2$]/3BrPA co-treatment, concurred to the selective toxicity of these molecules in neuroblastoma cells.

To explain the different susceptibility between SH-SY5Y and PCN towards [Cu(isaepy)$_2$]/3BrPA combined treatment, we measured the activity of the antioxidant enzymes SOD1, glutathione peroxidase and catalase in both cell types; however, no significant difference was evaluated (data not shown). Measurements of extracellular lactate (**Fig. 5E**) and several lines of evidence from the literature [42] indicate that PCN, such as many other non proliferating cell types, re-direct the majority of glucose, taken up from the extracellular space, towards the oxidative branch of the pentose phosphate pathway to generate NADPH, rather than utilize it as glycolytic substrate. This metabolic strategy should ensure a more “reducing” intracellular milieu, which better faces up to oxidative challenges. We then hypothesized that the shift of the glycolytic *versus* the pentose phosphate pathway, and in turn the levels of NADPH, could represent the determinant of the different sensitivity to [Cu(isaepy)$_2$]/3BrPA co-treatment observed in neuroblastoma and primary neurons. To verify this issue, PCN cells were grown in low glucose (LG)-containing milieu or, alternatively, in the presence of 1 μM of the glucose-6-phosphate dehydrogenase inhibitor dihydroepiandrosterone (DHEA), and then subjected to the combined treatment. **Fig. 6D** shows that, under both these conditions, PCN became susceptible to [Cu(isaepy)$_2$]/3BrPA treatment, with high percentages of cells displaying apoptotic nuclei. To assess whether oxidative stress took place under these conditions, we evaluated, by Western blot analyses, the content of protein carbonyls, one of the principal markers of occurred oxidative damage. SH-SY5Y showed a significant increase in protein carbonylation upon [Cu(isaepy)$_2$]/3BrPA treatment (**Fig. 6E**), confirming the high

production of ROS previously measured (**Fig. 6A**). Conversely, PCN did not display any relevant change in protein carbonyls, unless they were grown in LG or incubated with DHEA (**Fig. 6E**), conditions in which Western blot analyses showed an increase of phospho-AMPK, phospho-p38^{MAPK} and p53 immunoreactivity (**Fig. 6F**). Overall these data suggest that, even in PCN, cell death phenomena and oxidative damage downstream of [Cu(isaepy)$_2$]/3BrPA co-treatment were reasonably associated with the activation of AMPK/p38^{MAPK}/p53 signalling axis.

CONCLUSIONS

We previously demonstrated that [Cu(isaepy)$_2$] is a DLC-like molecule able to affect mitochondrial oxygen consumption and produce ROS, thereby resulting in a p53-mediated and AMPK-dependent apoptosis [28, 29]. On the basis of these results, here we have characterized that apoptosis proceeds *via* the intermediate action of p38^{MAPK}, thereby delineating an AMPK/p38^{MAPK}/p53 signalling axis as the principal route controlling [Cu(isaepy)$_2$]-induced apoptosis, with AMPK being the upstream sensor, p38^{MAPK} the mediator and p53 the final executioner of the death program. The inactivation of these proteins results in a significant reduction of the apoptotic extent, although this value decreased in dependence of the protein targeted, with the inhibition of AMPK, p38^{MAPK} or p53 resulting in 81, 52 or 32% decrease of cell death, respectively. These observations clearly suggest that other additional targets of either AMPK or p38^{MAPK} should exist and reasonably account for the remaining extent to reach the full recovery of cell viability.

In the searching for the upstream event triggering AMPK/p38^{MAPK}/p53 apoptotic axis, we demonstrated that energy deficiency is profoundly implicated in [Cu(isaepy)$_2$]-mediated toxicity. These data well correlated with the indication that the protective effects of RA towards [Cu(isaepy)$_2$] cytotoxicity depended on its capability to enhance glucose uptake [37]. This is in accordance with glucose addiction typical of tumour cells, which allows the occurrence of anabolic reactions and the acidification of the stromal environment by increasing lactate release. In regard to these metabolic changes, ATP depleting drugs (e.g. glycolytic inhibitors) have been recently exploited in cancer therapy. However, their use in single treatment did not gain the expected success, whereas their employment in combination with conventional chemotherapeutics affecting cellular homeostasis (e.g. redox or metabolic stressors) seems to be more achievable [43] Results obtained in this study indicated that the combined treatment with low doses of [Cu(isaepy)$_2$] and 3BrPA, a potent glycolytic inhibitor, was effective and selective, as it induced apoptosis in neuroblastoma cells without any significant toxicity towards differentiated PCN cells. 3BrPA can react with hexokinase II and succinate dehydrogenase [38-41], as well as the sulfhydryl and hydroxyl groups of other metabolic enzymes, such as pyruvate kinase [44], glutamate dehydrogenase [45], GAPDH [41, 46, 47] and 3-phosphoglycerate kinase [41], thereby inhibiting their activity by means of the formation of an irreversible covalent bond with its pyruvyl moiety. In particular, since hexokinase II is the specific mitochondria-located form of this enzyme in cancer cells, whose activity is pivotal for sustaining the high glycolytic rate of tumours (Warburg effect), the results obtained in this study give emphasis to the pivotal role of hexokinase II in tumor glycolysis.

Data from literature report that 3BrPA is also a ROS producer [48, 49]. Indeed, since 3BrPA inhibits hexokinase-mediated glucose phosphorylation, it is reasonable that not only cellular energetics, but also NADPH production *via* the pentose phosphate pathway could be hindered by treatment with 3BrPA. This assumption is consistent with the results obtained in SH-SY5Y, as well as in PCN in which the pentose phosphate pathway has been affected. Nevertheless, the observations that other DLCs affecting ATP production and cell viability (e.g., Rho123 and DQC) do not activate AMPK/p38^{MAPK}/p53 signalling pathway, let presume that the unavailability of energetic equivalents does not represent the sole determinant of [Cu(isaepy)$_2$] anti-tumour effects. Indeed, fuel substrates administration, as well as the increase of SOD activity in *h*SOD cells, only

partially inhibited AMPK/p38^{MAPK}/p53 axis activation and rescued cell viability in SH-SY5Y cells. Taken together these results suggest that energy deficiency is certainly involved in [Cu(isaepy)$_2$]-mediated cell death, but pro-oxidant conditions generated upon [Cu(isaepy)$_2$] treatment, and enhanced by 3BrPA administration, are strongly expected to control the strength of the downstream apoptotic response.

REFERENCES

1. Hardie, D.G. (2007) AMP-activated/SNF1 protein kinases: conserved guardians of cellular energy. Nat. Rev. Mol. Cell. Biol. **8**, 774-785.
2. Hardie, D.G., and Sakamoto, K. (2006) AMPK: a key sensor of fuel and energy status in skeletal muscle. Physiology **21**, 48-60.
3. Hue, L., Beauloye, C., Bertrand, L., Horman, S., Krause, U., Marsin, A.S., Meisse, D., Vertommen, D., and Rider, M.H. (2003) New targets of AMP-activated protein kinase. Biochem. Soc. Trans. **31**, 213-215.
4. Inoki, K., Zhu, T., and Guan, K.L. (2003) TSC2 mediates cellular energy response to control cell growth and survival. Cell **115**, 577-590.
5. Liang, J., Shao, S.H., Xu, Z.X., Hennessy, B., Ding, Z., Larrea, M., Kondo, S., Dumont, D.J., Gutterman, J.U., Walker, C.L., Slingerland, J.M., and Mills, G.B. (2007) The energy sensing LKB1-AMPK pathway regulates p27(kip1) phosphorylation mediating the decision to enter autophagy or apoptosis. Nat. Cell Biol. **9**, 218-224.
6. Ben Sahra, I., Laurent, K., Loubat, A., Giorgetti-Peraldi, S., Colosetti, P., Auberger, P., Tanti, J.F., Le Marchand-Brustel, Y., and Bost, F. (2008) The antidiabetic drug metformin exerts an antitumoural effect in vitro and in vivo through a decrease of cyclin D1 level. Oncogene **27**, 3576-3586.
7. Sarbassov, D.D., Ali, S.M., and Sabatini, D.M. (2005) Growing roles for the mTOR pathway. Curr. Opin. Cell Biol. **17**, 596-603.
8. Cao, C., Lu, S., Kivlin, R., Wallin, B., Card, E., Bagdasarian, A., Tamakloe, T., Chu, W.M., Guan, K.L., and Wan, Y. (2008) AMP-activated protein kinase contributes to UV- and H2O2 induced apoptosis in human skin keratinocytes. J. Biol. Chem. **283**, 28897-28908.
9. Okoshi, R., Ozaki, T., Yamamoto, H., Ando, K., Koida, N., Ono, S., Koda, T., Kamijo, T., Nakagawara, A., and Kizaki, H. (2008) Activation of AMP-activated protein kinase induces p53-dependent apoptotic cell death in response to energetic stress. J. Biol. Chem. **283**, 3979-3987.
10. Jones RG, Plas DR, Kubek S, Buzzai M, Mu J, Xu Y, Birnbaum, M.J., and Thompson, C.B. (2009) AMP-activated protein kinase induces a p53-dependent metabolic checkpoint. Mol. Cell **18**, 283-293.
11. Rattan, R., Giri, S., Singh, A.K., and Singh, I. (2005) 5-Aminoimidazole-4-carboxamide-1-beta-D-ribofuranoside inhibits cancer cell proliferation in vitro and in vivo via AMP-activated protein kinase. J. Biol. Chem. **280**, 39582-39593.
12. Meisse, D., Van de Casteele, M., Beauloye, C., Hainault, I., Kefas, B.A., Rider, M.H., Foufelle, F., and Hue, L. (2002) Sustained activation of AMP-activated protein kinase induces c-Jun N-terminal kinase activation and apoptosis in liver cells. FEBS Lett. **526**, 38-42.
13. Kefas, B.A., Cai, Y., Ling, Z., Heimberg, H., Hue, L., Pipeleers, D., and Van de Casteele, M. (2003) AMP-activated protein kinase can induce apoptosis of insulin-producing MIN6 cells through stimulation of c-Jun-N-terminal kinase. J. Mol. Endocrinol. **30**, 151-161.
14. Fruman, D.A., and Edinger, A.L. (2008) Cancer therapy: staying current with AMPK. Biochem. J. **412**, e3-5.
15. Huang, X., Wullschleger, S., Shpiro, N., McGuire, V.A., Sakamoto, K., Woods, Y.L., McBurnie, W., Fleming, S., and Alessi, D.R. (2008) Important role of the LKB1-AMPK pathway in suppressing tumourigenesis in PTEN-deficient mice. Biochem. J. **412**, 211-221.

16. Hwang, J.T., Kim, Y.M., Surh, Y.J., Baik, H.W., Lee, S.K., Ha, J., and Park, O.J. (2006) Selenium regulates cyclooxygenase-2 and extracellular signal-regulated kinase signalling pathways by activating AMP-activated protein kinase in colon cancer cells. Cancer Res. **66**, 10057-10063.
17. Memmott, R.M., Gills, J.J., Hollingshead, M., Powers, M.C., Chen, Z., Kemp, B., Kozikowski, A., and Dennis, P.A. (2008) Phosphatidylinositol ether lipid analogues induce AMP-activated protein kinase-dependent death in LKB1-mutant non small cell lung cancer cells. Cancer Res. 68, 580-588.
18. Pan, W., Yang, H., Cao, C., Song, X., Wallin, B., Kivlin, R., Lu, S., Hu, G., Di, W., and Wan, Y. (2008) AMPK mediates curcumin-induced cell death in CaOV3 ovarian cancer cells. Oncol. Rep. **20**, 1553-1559.
19. Kroemer, G., and Pouyssegur, J. (2008) Tumor cell metabolism: cancer's Achilles' heel. Cancer Cell **13**, 472-482.
20. Vander Heiden, M.G., Cantley, L.C., and Thompson, C.B. (2009) Understanding the Warburg effect: the metabolic requirements of cell proliferation. Science **324**, 1029-1033.
21. Dwarakanath, B.S. (2009) Cytotoxicity, radiosensitization, and chemosensitization of tumour cells by 2-deoxy-D-glucose in vitro. J. Cancer Res. Ther. **5**, S27-31.
22. Mathupala, S.P., Ko, Y.H., and Pedersen, P.L. (2009) Hexokinase-2 bound to mitochondria: cancer's stygian link to the "Warburg Effect" and a pivotal target for effective therapy. Semin. Cancer Biol. **19**, 17-24.
23. Modica-Napolitano, J.S., and Aprille, J.R. (2001) Delocalized lipophilic cations selectively target the mitochondria of carcinoma cells. Adv. Drug. Deliv. Rev. **49**, 63-70
24. Simons, A.L., Ahmad, I.M., Mattson, D.M., Dornfeld, K.J., and Spitz, D.R. (2007) 2-Deoxy-D-glucose combined with cisplatin enhances cytotoxicity via metabolic oxidative stress in human head and neck cancer cells. Cancer Res. **67**, 3364-3370.
25. Maschek, G., Savaraj, N., Priebe, W., Braunschweiger, P., Hamilton, K., Tidmarsh, G.F., De Young, L.R., and Lampidis, T.J. (2004) 2-deoxy-D-glucose increases the efficacy of adriamycin and paclitaxel in human osteosarcoma and non-small cell lung cancers in vivo. Cancer Res. **64**, 31-34.
26. Lampidis, T.J., Bernal, S.D., Summerhayes, I.C., and Chen, L.B. (1993) Selective toxicity of rhodamine 123 in carcinoma cells in vitro. Cancer Res. **43**, 716-720.
27. Kurtoglu, M., and Lampidis, T.J. (2009) From delocalized lipophilic cations to hypoxia: blocking tumor cell mitochondrial function leads to therapeutic gain with glycolytic inhibitors. Mol. Nutr. Food Res. **53**, 68-75.
28. Filomeni, G., Cerchiaro, G., Da Costa Ferreira, A.M., De Martino, A., Pedersen, J.Z., Rotilio, G., and Ciriolo, M.R.. (2007) Pro-apoptotic activity of novel Isatin-Schiff base copper(II) complexes depends on oxidative stress induction and organelle-selective damage. J. Biol. Chem. **282**, 12010-12021.
29. Filomeni, G., Piccirillo, S., Graziani, I., Cardaci, S., Da Costa Ferreira, A.M., Rotilio, G., and Ciriolo, M.R. (2009) The isatin-Schiff base copper(II) complex [Cu(isaepy)$_2$] acts as delocalized lipophilic cation, yields widespread mitochondrial oxidative damage and induces AMP-activated protein kinase-dependent apoptosis. Carcinogenesis **30**, 1115-1124.
30. Cerchiaro, G., Aquilano, K., Filomeni, G., Rotilio, G., Ciriolo, M.R., and Da Costa Ferreira, A.M. (2005) Isatin-Schiff base copper(II) complexes and their influence on cellular viability. J. Inorg. Biochem. **99**,1433-1440.
31. Riccardi, C., and Nicoletti, I. (2006) Analysis of apoptosis by propidium iodide staining and flow cytometry. Nat. Protoc. **1**, 1458-1461.
32. Filomeni, G., Desideri, E., Cardaci, S., Graziani, I., Piccirillo, S., Rotilio, G., and Ciriolo, M.R. (2010) Carcinoma cells activate AMP-activated protein kinase-dependent autophagy as survival response to kaempferol-mediated energetic impairment. Autophagy **6**, 202-216.

33. Cardaci, S., Filomeni, G., Rotilio, G., and Ciriolo, M.R. (2010) p38(MAPK)/p53 signalling axis mediates neuronal apoptosis in response to tetrahydrobiopterin-induced oxidative stress and glucose uptake inhibition: implication for neurodegeneration. Biochem. J. **430**, 439-451.
34. Lowry, O.H., Rosebrough, N.J., Farr, A.L., and Randall, R.J. (1951) Protein measurement with the Folin phenol reagent. J. Biol. Chem. **193**, 265-275.
35. Xia, Y., Ongusaha, P., Lee, S.W., and Liou, Y.C. (2009) Loss of Wip1 sensitizes cells to stress- and DNA damage-induced apoptosis. J. Biol. Chem. **284**,17428-17437.
36. Benard, G., and Rossignol, R. (2008) Ultrastructure of the mitochondrion and its bearing on function and bioenergetics. Antioxid. Redox Signal. **10**, 1313-1342.
37. Lee, Y.M., Lee, J.O., Jung, J.H., Kim, J.H., Park, S.H., Park, J.M., Kim, E.K., Suh, P.G., and Kim, H.S. (2008) Retinoic acid leads to cytoskeletal rearrangement through AMPK-Rac1 and stimulates glucose uptake through AMPK-p38^{MAPK} in skeletal muscle cells. J. Biol. Chem. 283, 33969-33974.
38. Geschwind, J.F., Ko, Y.H., Torbenson, M.S., Magee, C., and Pedersen, P.L. (2002) Novel therapy for liver cancer: direct intraarterial injection of a potent inhibitor of ATP production. Cancer Res. **62**, 3909-3913.
39. Geschwind, J.F., Georgiades, C.S., Ko, Y.H., and Pedersen, P.L. (2004) Recently elucidated energy catabolism pathways provide opportunities for novel treatments in hepatocellular carcinoma. Expert Rev. Anticancer Ther. **4**, 449-457.
40. Ko, Y.H., Pedersen, P.L., and Geschwind, J.F. (2001) Glucose catabolism in the rabbit VX2 model for liver cancer. Cancer Lett. **173**, 83-91.
41. Pereira da Silva, A.P., El-Bacha, T., Kyaw, N., dos Santos, R.S., da Silva, W.S., Almeida, F.C., Da Poian, A.T., and Galina, A. (2009) Inhibition of energy-producing pathways of HepG2 cells by 3-bromopyruvate. Biochem. J. **417**, 717-726.
42. Herrero-Mendez, A., Almeida, A., Fernández, E., Maestre, C., Moncada, S., and Bolaños, J.P. (2009) The bioenergetic and antioxidant status of neurons is controlled by continuous degradation of a key glycolytic enzyme by APC/C-Cdh1. Nat. Cell Biol. **11**, 747-752.
43. Tennant, D.A., Durán, R.V., and Gottlieb, E. (2010) Targeting metabolic transformation for cancer therapy. Nat. Rev. Cancer **10**, 267-277.
44. Acan, N.L., and Ozer, N. (2001) Modification of human erythrocyte pyruvate kinase by an active site-directed reagent: bromopyruvate. J. Enzyme Inhib. **16**, 457-464.
45. Baker, J.P., and Rabin, B.R. (1969) Effects of bromopyruvate on the control and catalytic properties of glutamate dehydrogenase. Eur. J. Biochem. **11**, 154-159.
46. Ganapathy-Kanniappan, S., Vali, M., Kunjithapatham, R., Buijs, M., Syed, L.H., Rao, P.P., Ota, S., Kwak, B.K., Loffroy, R., and Geschwind, J.F. (2010) 3-bromopyruvate: a new targeted antiglycolytic agent and a promise for cancer therapy. Curr. Pharm. Biotechnol. **11**, 510-517.
47. Ganapathy-Kanniappan, S., Geschwind, J.F., Kunjithapatham, R., Buijs, M., Vossen, J.A., Tchernyshyov, I., Cole, R.N., Syed, L.H., Rao, P.P., Ota, S., and Vali, M. (2009) Glyceraldehyde-3-phosphate dehydrogenase (GAPDH) is pyruvylated during 3-bromopyruvate mediated cancer cell death. Anticancer Res. **29**, 4909-4918.
48. Kim, J.S., Ahn, K.J., Kim, J.A., Kim, H.M., Lee, J.D., Lee, J.M., Kim, S.J., and Park, J.H. (2008) Role of reactive oxygen species-mediated mitochondrial dysregulation in 3-bromopyruvate induced cell death in hepatoma cells : ROS-mediated cell death by 3-BrPA. J. Bioenerg. Biomembr. **40**, 607-618.
49. Chen, Z., Zhang, H., Lu, W., and Huang, P. (2009) Role of mitochondria-associated hexokinase II in cancer cell death induced by 3-bromopyruvate. Biochim. Biophys. Acta. **1787**, 553-560.

FOOTNOTES

We gratefully acknowledge Palma Mattioli for her technical assistance in fluorescence microscopy and image analyses. This work was partially supported by grants from Ministero della

Salute; Ministero dell'Istruzione, dell'Università e della Ricerca (MIUR) and Associazione Italiana per la Ricerca sul Cancro (AIRC, Grant IG10636). The authors also gratefully acknowledge the Brazilian agencies Fundação de Amparo a Pesquisa do Estado de São Paulo (FAPESP, Grant 05/60596-8), Conselho Nacional de Desenvolvimento Científico e Tecnológico (CNPq, INCT Processos Redox em Biomedicina-Redoxoma), and Programma Esecutivo di Cooperazione Scientifica e Tecnologica Italia-Brasile (#490021/2008-5) for financial support to this work.

ABBREVIATIONS

AMPK, AMP-activated protein kinase; 3BrPA, 3-bromopyruvate; [Cu(isaepy)$_2$], bis[(2-oxindol-3-ylimino)-2-(2-aminoethyl)pyridine-N,N']copper(II); DHEA, dihydroepiandrosterone; DMEM, Dulbecco's modified Eagle's medium; DLCs, delocalized lipophilic cations; DMSO, dimethyl sulfoxide; DQC, dequalinium chloride; DTT, dithiotreitol; GAPDH, glyceraldehyde-3-phosphate dehydrogenase; H_2DCF-DA, 2',7'-dichlorodihydrofluorescein diacetate; JNK, c-Jun-N-terminal kinase; MAPK, mitogen activated protein kinase; 2-NBDG, 2-[N-(7-nitrobenz-2-oxa-1,3-diazol-4-yl) amino]-2-deoxy-D-glucose; OXPHOS, oxidative phosphorylation; PCN, primary cortical neurons; RA, retinoic acid; Rho123, rhodamine 123; ROS, reactive oxygen species; siRNA, small interference RNA; SOD, superoxide dismutase.

DISCLOSURE STATEMENTS

The authors declare no actual or potential conflicts of interest.

FIGURE LEGENDS

Figure 1. *p38^{MAPK} and p53 are activated downstream of AMPK upon treatment with [Cu(isaepy)$_2$].* **A.** Structure of [Cu(isaepy)$_2$]. **B.** SH-SY5Y cells were treated with 50 μM [Cu(isaepy)$_2$] or, as control, with equal volumes of DMSO. At indicated times, 30 μg of total protein extract was loaded onto each lane for the detection of basal and phospho-activated levels of AMPK and p38^{MAPK}, as well as p53. GAPDH was used as loading control. Western blots are from one experiment representative of three that gave similar results. **C.** SH-SY5Y cells were transfected with the dominant negative (T172A) mutant of AMPK (*AMPK D/N*) or with an empty vector (*mock*). After 48 h from transfection, cells were treated with 50 μM [Cu(isaepy)$_2$] for 24 h or, as control, with equal volumes of DMSO, washed and stained with propidium iodide. Analyses of the extent of apoptosis (*SubG1*) were performed by a FACScalibur instrument and percentages of staining-positive cells were calculated using WinMDI version 2.8 software. Cell cycle plots reported are from a typical experiment done in triplicate out of five that gave similar results. **D.** Mock and AMPK D/N SH-SY5Y cells were treated with 50 μM [Cu(isaepy)$_2$] for 6 and 12 h or, as control, with equal volumes of DMSO. 30 μg of total protein extract was loaded onto each lane for the immunodetection of phospho-AMPK, phospho-p38^{MAPK} and p53. GAPDH was used as loading control. Western blots are from one experiment representative of three that gave similar results. **E.** Mock and AMPK D/N SH-SY5Y were treated for 6 h with 50 μM [Cu(isaepy)$_2$], washed, fixed in 4% paraformaldehyde and permeabilized. Phospho-p38^{MAPK} and p53 were visualized upon staining with specific antibodies and further probed with Alexa fluor®-488 and Alexa fluor®-568-conjugated secondary antibodies, respectively. To visualize nuclei, cells were also incubated with the cell permeable DNA dye Hoechst 33342. Images reported are from one experiment out of three that gave similar results. Untreated parental SH-SY5Y cells (*DMSO*) were used as control.

Figure 2. *Inhibition of p38^{MAPK} activation results in a decrease of p53 accumulation and apoptosis induced by [Cu(isaepy)$_2$].* **A.** SH-SY5Y cells were transfected with two siRNAs against p38^{MAPK} (*sip38$_1$* or *sip38$_2$*) or with a scramble siRNA sequence (*siScr*). After 12 h, cells were treated for further 24 h with 50 μM [Cu(isaepy)$_2$] or, as control, with equal volumes of DMSO, stained with

propidium iodide and analyzed cytofluorometrically for apoptotic extent. Data are expressed as % of SubG1 (apoptotic) cells and represent the mean ± SD of n = 4 independent experiments. *p < 0.05; **p < 0.01. **B.** siScr and sip38$_1$ cells were treated with 50 μM [Cu(isaepy)$_2$] or, as control, with equal volumes of DMSO. At indicated times, 30 μg of total protein extract was loaded onto each lane for the immunodetection of phospho-p38^{MAPK} and p53. GAPDH was used as loading control. Western blots are from one experiment representative of three that gave similar results. **C.** SH-SY5Y cells were transfected with a kinase mutant form of p38^{MAPK} (*p38-KM*) or with an empty vector (*mock*). After 48 h from transfection, mock and p38-KM cells were treated for 24 h with 50 μM [Cu(isaepy)$_2$] or, as control, with equal volumes of DMSO, stained with propidium iodide and analyzed cytofluorometrically for apoptotic extent. Data are expressed as % of SubG1 (apoptotic) cells and represent the mean ± SD of n = 4 independent experiments. **p < 0.01. **D.** Mock and p38-KM cells were treated with 50 μM [Cu(isaepy)$_2$] or, as control, with equal volumes of DMSO. At the indicated times, 30 μg of total protein extract was loaded onto each lane for the immunodetection of phospho-p38^{MAPK} and p53. GAPDH was used as loading control. Western blots are from one experiment representative of three that gave similar results.

Figure 3. *Increased availability of fuel supplies inversely correlates with the activation of AMPK/p38^{MAPK}/p53 signalling axis and apoptosis induced by [Cu(isaepy)$_2$].* **A.** SH-SY5Y cells were treated for 24 h with 50 μM [Cu(isaepy)$_2$] or, as control, with equal volumes of DMSO, in medium supplemented with 30 mM glucose, 10 mM pyruvate or 10 mM methyl succinate (*Me-succ*), stained with propidium iodide and analyzed cytofluorometrically for apoptotic extent. As control for fuel supplies administration, equal volumes of PBS were added to cell culture media. Data are expressed as % of SubG1 (apoptotic) cells and represent the mean ± SD of n = 4 independent experiments. *p < 0.05; **p < 0.01 with respect to [Cu(isaepy)$_2$]-treated cells. $^{\dagger}p$ < 0.05; $^{\dagger\dagger}p$ < 0.01 with respect to [Cu(isaepy)$_2$]-treated cells incubated with pyruvate. **B.** Alternatively, at the indicated times, 30 μg of total protein extract was loaded onto each lane for the immunodetection of the phospho-activated levels of AMPK and p38^{MAPK}, as well as p53. GAPDH was used as loading control. Western blots are from one experiment representative of three that gave similar results. Densitometric analyses of phospho-AMPK, phospho-p38^{MAPK}, p53 and GAPDH were calculated using Quantity One Software. Data are expressed as P-AMPK/GAPDH, P-p38^{MAPK}/GAPDH, p53/GAPDH ratios and represent the means ± SD. *p < 0.05; **p < 0.01; ***p < 0.001. **C.** SH-SY5Y cells were grown for two weeks in the presence 20 μM retinoic acid (*RA*) or, as control, with equal volumes of DMSO. Afterwards, they were incubated with 100 μM 2-NBDG for 1 h, washed to stop 2-NBDG uptake, collected and fluorescence analyzed cytofluorometrically by a WinMdi 2.8 software. Data are expressed as % of 2-NBDG positive cells and represent the mean ± SD of n = 3 independent experiments. ***p < 0.001. **D.** RA-differentiated cells were treated with 50 μM [Cu(isaepy)$_2$] or, as control, with equal volumes of DMSO. At the indicated times, 30 μg of total protein extract was loaded onto each lane for the immunodetection of the phospho-activated levels of AMPK and p38^{MAPK}, as well as p53. GAPDH was used as loading control. Western blots are from one experiment representative of three that gave similar results.

Figure 4. *The DLCs DQC and Rho123 induce apoptosis independently on the activation of AMPK/p38^{MAPK}/p53 signalling axis.* **A.** SH-SY5Y cells were treated for 24 h with 100 μM dequalinium chloride (*DQC*), rhodamine 123 (*Rho123*) or, as control, with equal volumes of PBS or DMSO, and next washed and stained with propidium iodide. Analyses of the extent of apoptosis (*SubG1*) were calculated using WinMDI version 2.8 software. Cell cycle plots reported are from a typical experiment done in triplicate out of five that gave similar results. **B.** Alternatively, at the indicated times, 30 μg of total protein extract was loaded onto each lane for the immunodetection of the phospho-activated levels of AMPK and p38^{MAPK}, as well as p53. GAPDH was used as loading control. Western blots are from one experiment representative of three that gave similar results. **C.**

Mock, AMPK D/N cells, and parental SH-SY5Y incubated with 10 μM of the pharmacological inhibitor of p53, pifithrin-α (*pif-α*) or, as control, with equal volumes of DMSO, were treated for 24 h with 100 μM DQC or Rho123, stained with propidium iodide and analyzed cytofluorometrically for apoptotic extent. Data are expressed as % of SubG1 (apoptotic) cells and represent the mean ± SD of n = 4 independent experiments.

Figure 5. *3BrPA enhances the activation of AMPK/p38^{MAPK}/p53 signalling axis and apoptosis induced by [Cu(isaepy)$_2$].* **A.** SH-SY5Y cells were treated with 10 μM [Cu(isaepy)$_2$] or, as control, with equal volumes of DMSO in the presence or absence of 10 μM 3-bromopyruvate (*3BrPA*, dissolved in PBS) for 24 h, stained with propidium iodide and analyzed cytofluorometrically for apoptotic extent. Data are expressed as % of SubG1 (apoptotic) cells and represent the mean ± SD of n = 4 independent experiments. ***$p < 0.001$. **B.** Alternatively, after 6 h of treatment, 30 μg of total protein extract was loaded onto each lane for the immunodetection of the phospho-activated levels of AMPK and p38^{MAPK}, as well as p53. GAPDH was used as loading control. Western blots are from one experiment representative of three that gave similar results. **C.** Primary cortical neurons (PCN) were treated with 10 μM [Cu(isaepy)$_2$] or, as control, with equal volumes of DMSO in the presence or absence of 10 μM 3BrPA for 24 h,washed, fixed in 4% paraformaldehyde and permeabilized. Cleaved caspase-3 was visualized upon staining with a specific antibody and further probed with Alexa fluor®-568-conjugated secondary antibody. To visualize nuclei, cells were also incubated with the cell permeable DNA dye Hoechst 33342. Images reported are from one experiment out of five that gave similar results, the percentages of which are shown in **D.**, along with the extent of apoptotic SH-SY5Y cells measured upon the combined treatment (*Black bar*) Data are expressed as % of cells displaying apoptotic nuclei or cleaved caspase-3 and represent the mean ± SD of n = 4 independent experiments. **E.** SH-SY5Y cells and PCN were treated with 10 μM [Cu(isaepy)$_2$] or, as control, with equal volumes of DMSO in the presence or absence of 10 μM 3BrPA for 6 h. Cell media were then collected and lactate determined spectrophotometrically following the reduction of NAD^+ at 340 nm. Data are expressed as nmoles of lactate/ml and represent the mean ± SD of n = 3 independent experiments. *$p < 0.05$; **$p < 0.01$.

Figure 6. *Oxidative conditions contribute to AMPK/p38^{MAPK}/p53 signalling axis and apoptosis induced by the combination of [Cu(isaepy)$_2$] and 3BrPA.* **A.** SH-SY5Y cells and PCN were treated with 10 μM [Cu(isaepy)$_2$] or, as control, with equal volumes of DMSO in the presence or absence of 10 μM 3BrPA (dissolved in PBS) for 6 h and incubated with 50 μM H_2DCF-DA. Cells were then washed with PBS and ROS production was analyzed cytofluorometrically. Data are expressed as % of DCF^+ cells and represent the mean ± SD of n = 4 independent experiments. *$p < 0.05$; **$p < 0.01$; ***$p < 0.001$. **B.** Parental or SOD1 overexpressing (*hSOD*) SH-SY5Y cells were treated with 10 μM [Cu(isaepy)$_2$] or, as control, with equal volumes of DMSO in the presence of 10 μM 3BrPA for 24 h, stained with propidium iodide and analyzed cytofluorometrically for apoptotic extent. Data are expressed as % of SubG1 (apoptotic) cells and represent the mean ± SD of n = 4 independent experiments. **$p < 0.01$. **C.** Alternatively, after 6 h of treatment, 30 μg of total protein extract was loaded onto each lane for the immunodetection of the phospho-activated levels of AMPK and p38^{MAPK}, as well as p53. GAPDH was used as loading control. Western blots are from one experiment representative of three that gave similar results. **D.** PCN were grown in medium containing 5 mM glucose (low glucose: *LG*), or in the presence of 1 μM of the glucose-6-phosphate inhibitor dihydroepiandrosterone (*DHEA*) or, as control, with equal volumes of DMSO. PCN were then subjected to the combined treatment with 10 μM [Cu(isaepy)$_2$] and 3BrPA for 24 h, washed, fixed in 4% paraformaldehyde and permeabilized. Apoptotic nuclei were visualized upon staining with the cell permeable DNA dye Hoechst 33342. Images reported are from one experiment out of five that gave similar results, the percentages of which are shown below. Data are expressed as % of

cells displaying apoptotic nuclei and represent the mean ± SD of n = 4 independent experiments. ***$p < 0.001$. **E.** PCN were grown in *LG*-containing medium or in the presence of 1 μM DHEA or, as control, with equal volumes of DMSO and then subjected to the combined treatment with 10 μM [$Cu(isaepy)_2$] and 3BrPA. 30 μg of total protein extract was loaded onto each lane for the immunodetection of protein carbonyls. Carbonyls from SH-SY5Y treated with the combined treatment were also shown. GAPDH was used as loading control. Densitometric analyses were calculated using Quantity One Software. Data are expressed as carbonyls/GAPDH ratio and represent the means ± SD. *$p < 0.05$; **$p < 0.01$; ***$p < 0.001$. **F.** PCN were grown in *LG*-containing medium or in the presence of 1 μM DHEA or, as control, with equal volumes of DMSO and then subjected to the combined treatment with 10 μM [$Cu(isaepy)_2$] and 3BrPA. 30 μg of total protein extract was loaded onto each lane for the immunodetection of the phospho-activated levels of AMPK and $p38^{MAPK}$, as well as p53. GAPDH was used as loading control. Western blots are from one experiment representative of three that gave similar results.

Biochemical Journal Immediate Publication. Published on 06 May 2011 as manuscript BJ20110510

FIGURE 1

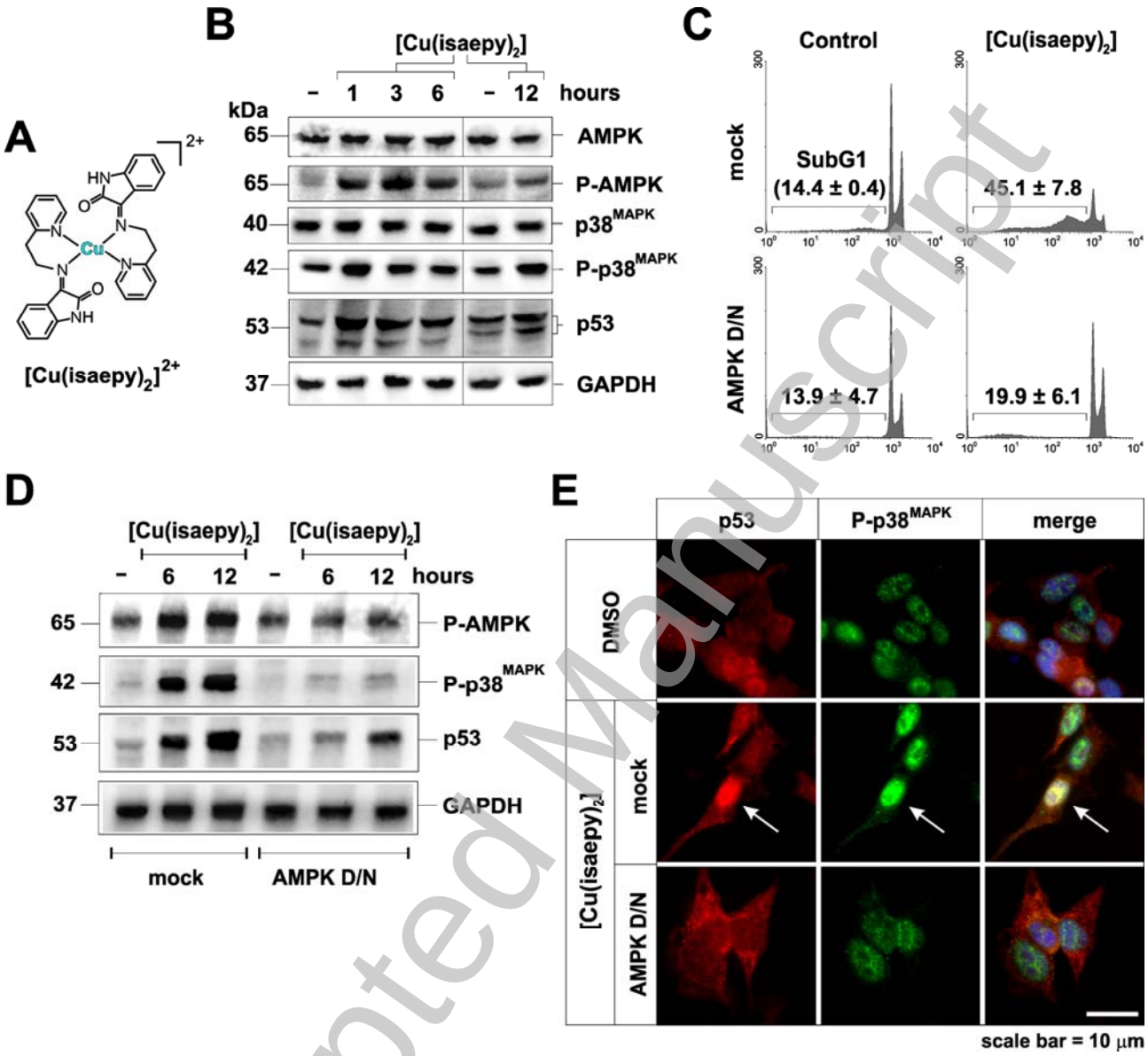

FIGURE 2

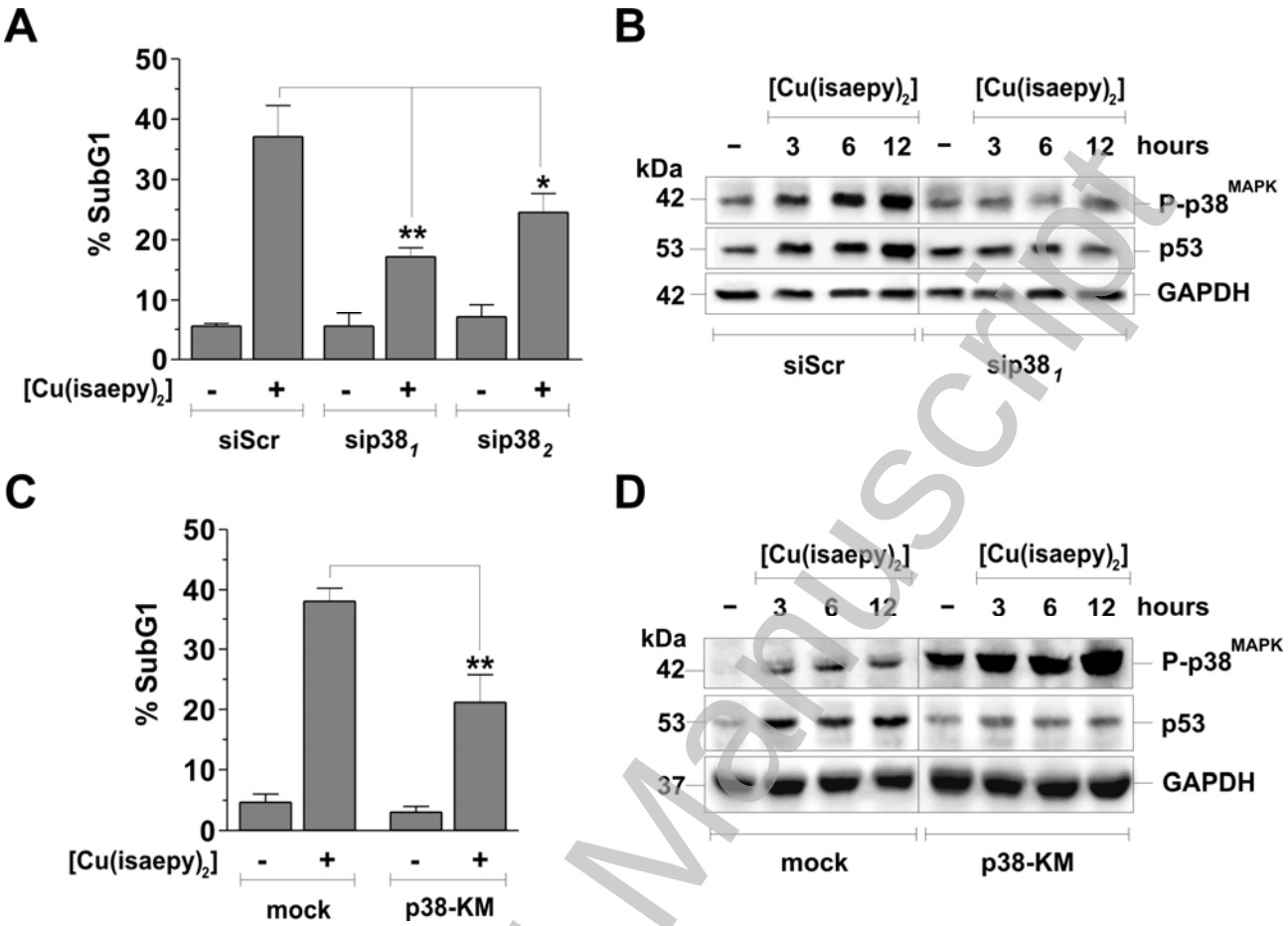

FIGURE 3

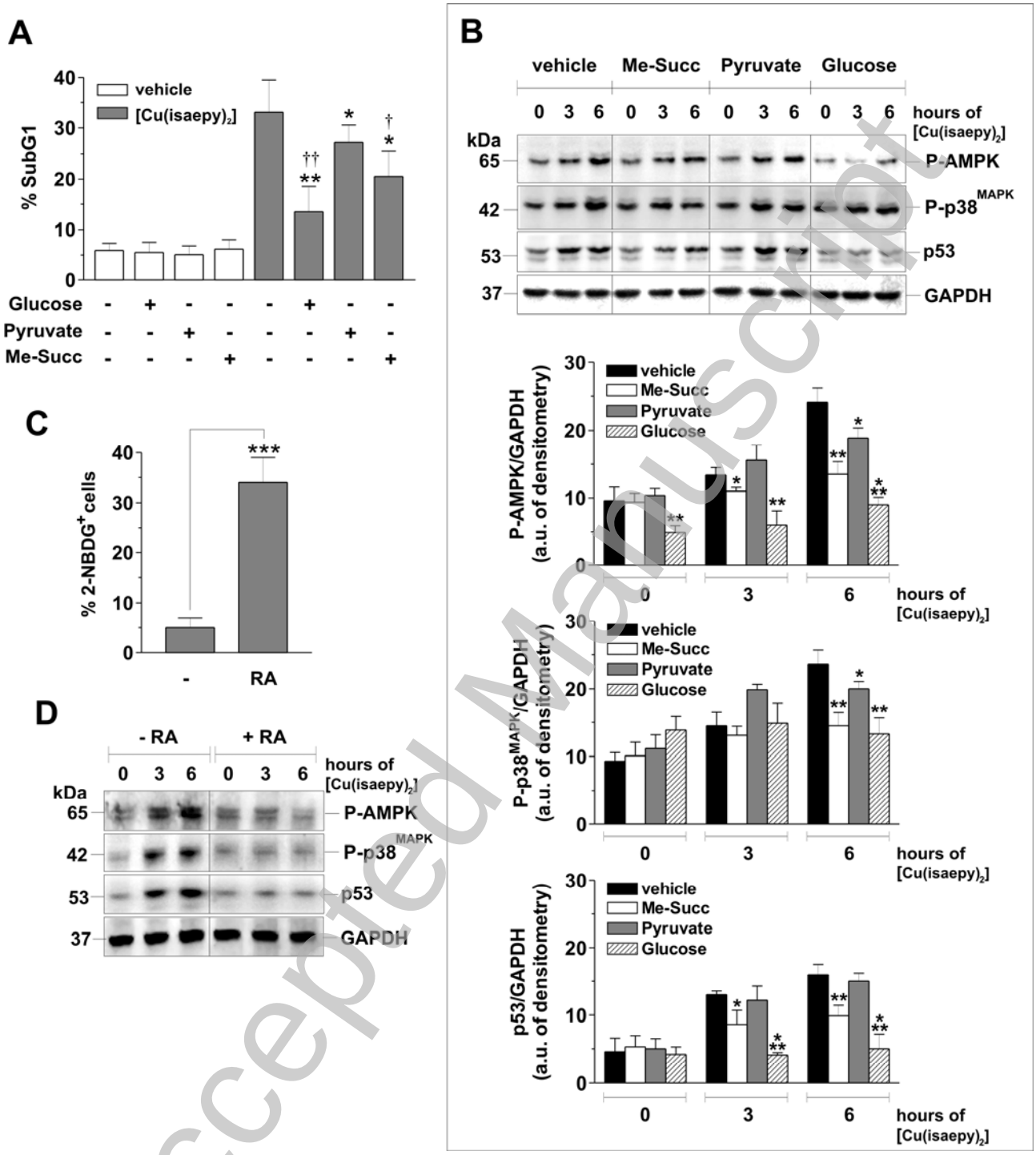

Biochemical Journal Immediate Publication. Published on 06 May 2011 as manuscript BJ20110510

FIGURE 4

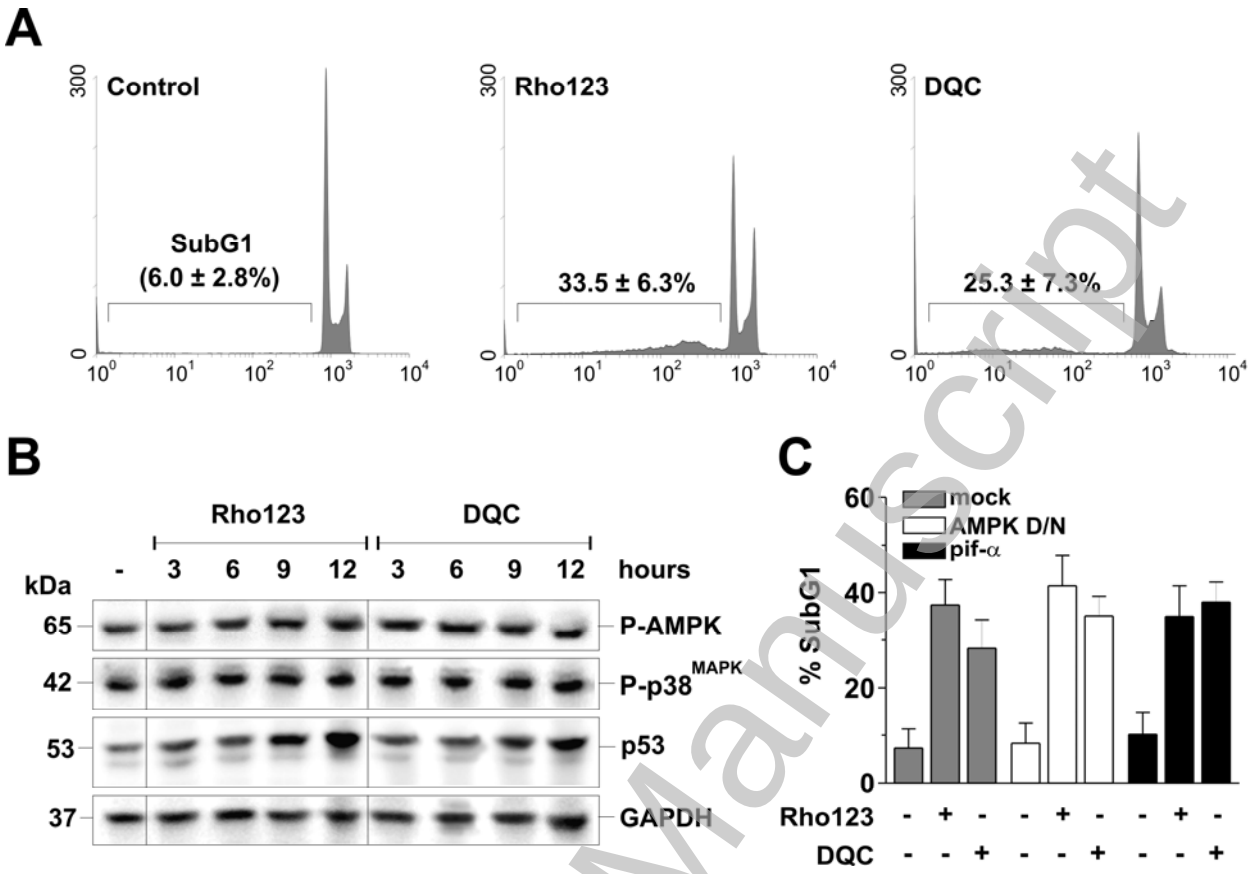

FIGURE 5

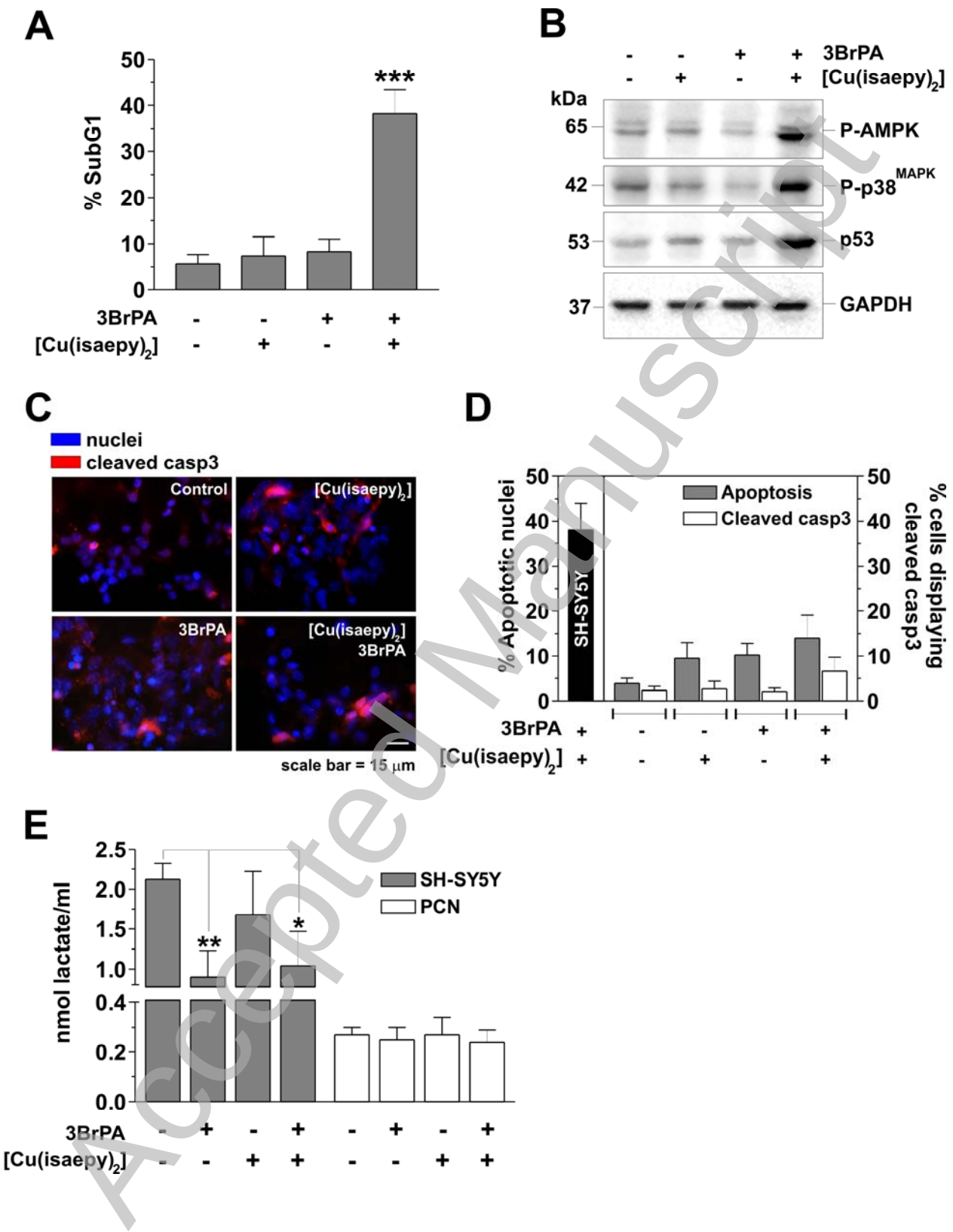

Biochemical Journal Immediate Publication. Published on 06 May 2011 as manuscript BJ20110510

FIGURE 6